heritage

*Article*

# New Insight on Medieval Painting in Sicily: The Virgin *Hodegetria* Panel in Monreale Cathedral (Palermo, Italy)

**Maria Letizia Amadori [1,*], Valeria Mengacci [1], Mauro Sebastianelli [2], Bruno Pignataro [3], Simonpietro Agnello [3], Paolo Triolo [1] and Claudia Pellerito [3]**

[1] Department of Pure and Applied Sciences, University of Urbino, p.zza Rinascimento 6, 61029 Urbino, Italy; valeria.mengacci@uniurb.it (V.M.); paolo.triolo@uniurb.it (P.T.)
[2] Soprintendenza BB.CC.AA., Regione Sicilia, via Garibaldi 41, 90133 Palermo, Italy; mauro.sebastianelli@regione.sicilia.it
[3] Department of Physics and Chemistry E. Segrè, University of Palermo, v.le delle Scienze, Parco d'Orleans, 90128 Palermo, Italy; bruno.pignataro@unipa.it (B.P.); simonpietro.agnello@unipa.it (S.A.); claudia.pellerito@unipa.it (C.P.)
* Correspondence: maria.amadori@uniurb.it

**Abstract:** The Virgin *Hodegetria*, located in the Cathedral of *Santa Maria Nuova* in Monreale, near Palermo (Italy), probably dating the first half of the 13th century, is one of the earliest examples of medieval panel painting in Sicily. A diagnostic campaign was carried out on the panel aiming to identify the constituting materials and the executive technique, as well as to assess the state of conservation for supporting the methodological choice of the restoration intervention. Both non-invasive (X-ray radiography, digital microscope, multispectral imaging, ED-X-ray fluorescence) and micro-invasive (polarised light microscopy, ESEM-EDX, ATR-FTIR spectroscopy and micro-Raman spectroscopy) analyses were performed. According to the results, the executive technique followed the 13th–14th-century Italian painting tradition. A complex structure was applied on the wooden support, consisting of a double layer of canvas and several ground layers of gypsum and glue-based binder. The underdrawing was made by a brush using carbonaceous black pigment. The original palette includes red ochre, red lead, azurite, carbon black and bone black. During the several restorations, mercury-based red, indigo, smalt blue, orpiment and synthetic mars were used. The original silver leaf of the frame was covered with red tin-based lake and subsequently regilded with gold leaf. Proteinaceous and oil binders were also detected.

**Keywords:** virgin *Hodegetria* panel; Monreale Cathedral; microscopy; spectroscopy



**Citation:** Amadori, M.L.; Mengacci, V.; Sebastianelli, M.; Pignataro, B.; Agnello, S.; Triolo, P.; Pellerito, C. New Insight on Medieval Painting in Sicily: The Virgin *Hodegetria* Panel in Monreale Cathedral (Palermo, Italy). *Heritage* **2023**, *6*, 4692–4709. https://doi.org/10.3390/heritage6060249

Academic Editors: Teresa Ferreira, Patrícia Moita, Cristina Galacho and Mafalda Costa

Received: 12 May 2023
Revised: 1 June 2023
Accepted: 2 June 2023
Published: 6 June 2023



## 1. Introduction

The Virgin *Hodegetria* (Figure 1a,b), called both *Madonna Bruna* and *della Negra* or Icon of William II [1], is one of the earliest examples of medieval painting in Sicily. The panel is currently kept in the Cathedral of *Santa Maria Nuova*, Monreale, which was listed in 2015 as a UNESCO World Heritage site. For a long time, it was considered an icon but recent research [1,2] recognised that it represents a Romanesque panel strictly linked to the Greek manner, dating from the end of the 12th and the first half of the 13th century. Therefore, because of the strong Byzantine matrix and its large size (169 × 131 × 3 cm), it is reputed as an altarpiece image proportionate to the gigantism of the Benedictine Cathedral.

According to the tradition, the panel was commissioned for private devotion by King William II of Sicily (1153–1189), founder of the Benedictine Cathedral of *Santa Maria Nuova*, who was one of the most popular Norman kings, called the Good, and the last descendant of the Altavilla family [3,4].

The panel, attributed to an unknown artist, is a variant of the classic *Hodegetria* [5]: it represents the Virgin holding the Christ Child on her left side while pointing to him with her right hand, as a symbolic representation of the religious text. The shaping of

the Sicilian *Hodegetria* face and the lines delimiting the eyelids, nose and mouth are both similar to the icons of the Virgin *Eleousa* [6] and the Virgin *Enkleistra* [7], both made by the Constantinopolitan painter Theodoros Apsevdis (1183) [6,7], and the Archangel Michael of the Monastery of Agios Chrysostomos in Koutzovendi (about 1200) [7]. These peculiarities recall popular models used in wall paintings and icons of the 12th and 13th centuries [8]. The Cypriot matrix of the image is attested by the presence of an original silver background and the relief decorations [9]. These techniques, introduced by the Byzantine iconographers, became widespread in the Cypriot and Sinaitic areas, and later in Catalonia and Tuscany [10]. Moreover, elements such as the two circular lamps on the forehead of the Child, the haloes with a spiral motif, the edges, the stars of the *maphorion*, the fibula at the base of the Virgin's neck or the crossed legs of the Son derive from oriental models acquired and modified in the West areas [9].


**Figure 1.** The Virgin *Hodegetria* panel painting (first half of 13th century): (**a**) before the restoration, with ED-XRF measurement points (in white colour: from 1 to 23) and sampling areas (in pale blue colour: from MOM-A to MOM-H); (**b**) PLM micrography of the wooden sample MOM-H; (**c**) detail of a lacuna showing the *impannatura* consisting of two linen cloths with plain weave.

Despite its doubtful nature (both an icon and a panel), the care of this type of artefact takes particular attention to its function: indeed, like other icons, the Virgin *Hodegetria* panel is held in devotion and is venerated during ritual practices. For these reasons, several regilding and different restoration interventions required a diagnostic campaign before planning the conservation project to identify the original iconography and the stylistic specificities of the masterpiece of Monreale [11,12].

*Previous Studies*

The icons are generally flat panels depicting a holy person or object such as Jesus, the Virgin Mary, saints, angels, or the cross [13]. They were widely present in the Byzantine world and, subsequently, the Christian traditions of Eastern Orthodoxy used them to evoke veneration and educate the masses [13]. From the historical and artistic point of view, the icon traditions have influenced many of the areas governed by the Byzantine Empire, and this is also due to the remarkable ease of movement of these artefacts [14]. Demus [15] suggested that from the 12th century, the strong revival of painting on wood (panels, altarpieces and polyptychs later) represents icon adaptations both to different structures of Western churches (often without iconostasis) and the different liturgy. Belting argued

that it is not clear where the modern panel painting comes from in the form of a devotional image, which developed in the context of late medieval mysticism collectors [14].

According to Byzantine tradition, a wooden panel image of the Virgin *Hodegetria* was attributed to the miraculous creation of the evangelist Saint Luke, who painted it around the twelfth century. In this composition, the Virgin cradles the Christ Child in her left arm and points toward him with her right hand [16]. In the 5th century, it was sent to Constantinople from Jerusalem as a major Christian relic.

The *Hodegetria* image was extremely popular in the East and had a strong impact on representations of the Virgin and Christ Child in Western Europe during the Middle Ages and Renaissance [17]. In West areas, mostly in Italy, the technique developed for medieval panels was so similar to that used in Byzantine production to recognise a new trend called the "Greek Manner" [13] from Renaissance writers such as Giorgio Vasari [18]. Probably the 13th-century painters mixed Byzantine characters of the half-length Madonna and Child with Western Marian elements, thus creating new variants that no longer correspond to the Byzantine ones [19,20]. Furthermore, Schmidt attested [19] that an icon is not an altarpiece, as it was not created as stable altar equipment. Therefore, the arrangement of Marian icons above the high altar, which is found in many Italian churches, should be considered post-medieval.

The techniques for preparing the boards and the constituting materials, as well as the techniques of medieval icons and panels, are widely described in historical sources and deeply studied ([21–29] and references therein).

In the Byzantine period, the palette of Greek icons was limited and consisted of earth pigments (yellow and red ochre, hematite, *caput mortuum*, green earth), lead white, cinnabar and carbon black [30,31]. Azurite mixed with indigo, kermes lake and safflower were detected in the 13th-century Italian panel painting depicting a Madonna and Child [32]. In the dossal of Meliore, a panel of the 13th century, in addition to the already mentioned pigments, green lake, ultramarine blue and Pb–Sn yellow were detected [25]. Byzantine and Early Christian icons and medieval panel paintings were traditionally produced using egg tempera [22,33–36]. Non-invasive analyses on Byzantine Albanian icons (14th and 15th centuries) revealed the occurrence of a tempera technique and the use of lead white, calcium carbonate, cinnabar, red and yellow ochre, red lead, brown earth, Cu-based pigments, indigo, ivory/bone black and realgar/orpiment [37]. Generally, proteinaceous materials and oils were detected in byzantine and post-byzantine paintings, due to the influence of Western art [31]. In post-Byzantine icons, azurite and Cu-based resinate were identified [30,34,38]. In Cretan icons, dated between the 15th and 17th centuries [39], the extensive use of kermes lake was found, while in later icons, cochineal dye was used. Madder and indigoid dyes were also used as colouring matters or in mixtures with inorganic pigments, such as red ochre, cinnabar, minium, azurite lead white and carbon black [39]. Egg yolk, oil and natural resin were identified in the same icons [40]. In their interesting review, Sotiropoulou and Daniilia [30] discussed the addition of oil in the egg binder or a possible dilution of the egg binder to obtain a transparent and shining effect as an influence of the West technique on the Greek icons.

During the Middle Ages and Early Renaissance, gilding and imitation of gold leaves were widely used to cover the front and sides of wooden panels and icons [29] with the aim of expressing the immaterial divine world and the holiness of the represented figures. The metal leaf was usually applied on siccative oil film (linseed oil) or using proteinaceous substances (glue, white egg) plus other components (pigments, water, white wine) ([22,25,29] and references therein) or on bolus [41].

Sometimes oleo-resinous varnishes were applied on silver leaf both for gilding imitation and to avoid the oxidation phenomena [28]. In many cases, throughout time, the original gilding was removed or retouched [42] using surrogate gold or orpiment [32].

## 2. Materials and Methods

Non-invasive investigations were first carried out in order to collect as much information as possible on the Virgin *Hodegetria* panel. As a second step, after carefully collecting

a series of representative micro-samples (Figure 1a), micro-invasive investigations were carried out with the aim of completing the diagnostic campaign.

### *2.1. X-ray Radiography (XRR)*

X-ray radiography was performed with a Villa X-Ray instrument equipped with an Apollo DFR table. Digital radiographic acquisitions were mosaicked and automatically recorded [43] using a CR control Fuji (FCR) digital imaging system (range 15–40 kV, current 0.5 mA, detector size 350 × 430 mm, SDD 1500 mm).

### *2.2. Digital Microscopy (OM)*

In situ preliminary observations were carried out with a Dino-Lite Universal USB digital microscope (interface USB 2.0, sensor CMOS 5 Megapixel, equipped with polariser anti-reflection and IR cut-filter > 650 nm), directly connected to PC. Images were acquired at 50× and 220× magnifications.

### *2.3. Imaging Techniques*

Multispectral imaging was carried out in the visible range (diffuse light photography and macro photography) and IR range (IR digital photography) using a Nikon D800 digital camera, with a 35.9 × 24 mm SLR 36.3 MP CMOS (7360 × 4912 Pixels) with a Nikkor 50 mm 1:1.8 G lens for visible light; using a Fuji IS Pro II IRUV with a 23.7 mm × 15.6 mm APS-C Super CCD (4256 × 2848 Pixel) with a Nikkor 28 mm f2.8 D coupled with PECA #910 (87C) IR filter and PECA #914 (89B) IR filters. Visible and IR light set: n.2 Osram Nitra phot bm 500 lamps.

Infrared false colour (IRFC) was processed to identify metameric pigment in Adobe Photoshop. Colour correction was made in Adobe Lightroom on RAW files. Colorimetric references: X-rite Colour chart Classic, parameterised on Spectral on 99% tab by Lab sphere [44,45], HD mosaicing was processed in Adobe Photoshop.

UV fluorescence was carried out with a Nikon D60 equipped with a Nikkor 18–55 DX G lens. UV fluorescence light set: n.2 UVP B-100AP ultraviolet black light lamps (100 W).

### *2.4. Energy Dispersive X-ray Fluorescence Spectrometry (ED-XRF)*

Energy Dispersive X-Ray fluorescence analysis was carried out using an Oxford Instrument X-Met 8000 energy dispersive handheld spectrometer, with an X-Flash SDD detector and 6 mm diameter spot, with an Rh target X-ray tube operating both at 8 kV, 50 μA and 40 kV, 8 μA. The first operating condition is particularly sensitive to light elements (from about Al) and the second to heavier ones, including Sn, Sb and Ba K-lines. The measurement time was 60 s: 44 s at 8 kV and 16 s at 40 kV. Data were processed using Artax software. Twenty-two points (Table S1), representative of the entire chromatic palette, were selected and analysed.

### *2.5. Sampling*

Eight representative micro fragments were carefully collected from the front and back of the panel. The micro-samples were collected close to gaps in order to preserve the reading of the painting. Sample MOM-A was collected from the front of the panel and represents the painting stratigraphy, sample MOM-B was taken from the frame in the gilding area, sample MOM-C was sampled in the background, MOM-D and MOM-F are related to the overpainted sky-bottom area, MOM-E is a sample collected from Virgin's blue sleeve, MOM-G was sampled from the underdrawing and MOM-H is a wooden sample collected from the back. The samples MOM-A and MOM-B were embedded in an epoxy resin and carefully polished after curing the resin with progressively finer paper to be made into cross-sections; the wooden sample MOM-H A was prepared following standard procedures [46], while the other samples were analysed without any preparation. The location (Figure 1a), the description of the samples and the analyses performed are indicated in Table 1.

**Table 1.** Description of micro-samples collected from Virgin *Hodegetria*.

| Sample Code | Sampling Area | Sample Description | Investigation |
|---|---|---|---|
| MOM-A | Maphorion of the Virgin | Red hue | PLM, ESEM-EDX, ATR-FTIR, μ-Raman |
| MOM-B | Table frame, front | Gilding | PLM, ESEM-EDX, ATR-FTIR |
| MOM-C | Background | Gilding | PLM, ESEM-EDX |
| MOM-D | Background near the angel, left side | Blue-red repainting | ESEM-EDX |
| MOM-E | Virgin's sleeve | Blue hue | μ-Raman |
| MOM-F | Background near, right side | Blue repainting | μ-Raman |
| MOM-G | Right shoulder of the Virgin | Black underdrawing | μ-Raman |
| MOM-H | Back of the panel | Wood support | PLM |

### *2.6. Polarised Light Microscopy (PLM)*

Polarised light microscopy observations were carried out with a BX51 Olympus microscope equipped with fixed ocular (magnification 10×) and objective lenses with different magnification (5×, 10×, 20×, 50×) directly connected to an Olympus SC50 camera and to Stream Basic software for image acquisition. The painting samples (MOM-A and MOM-B; Table 1) were embedded into a transparent polyester resin support, then cross-sectioned and polished. The resin blocks were polished successively with finer grades of micromesh abrasive cloths until the cross-section surfaces became smooth. The cross-sections were observed in reflected light to define colours, typology, thickness and the painting technique. Transmitted light observations on a thin section allowed the identification [46] of the wooden sample (MOM-H; Table 1).

### *2.7. Environmental Scanning Electron Microscopy and Energy Dispersive X-ray Spectrometry (ESEM/EDX)*

The investigations were carried out using Philips Quanta FEI 200 Environmental Scanning Electron Microscope equipped with an energy-dispersive X-ray spectrometer by Link Analytical Oxford (Link, UK), model 6103. Cross-sections (MOM-A and MOM-B) and specimens (MOM-C and MOM-D) were investigated by setting them on conductive double-sided carbon tabs. The analyses were carried out at an acceleration voltage from 15 to 20 kV with a variable working distance, 40 μA filament current and 100 s lifetime.

### *2.8. Fourier Transform Infrared Spectroscopy*

A Thermo Nicolet iS10 FTIR spectrophotometer equipped with Thermo Continuum IR microspectrophotometer and with a micro-ATR device with silicon crystal (Thermo Scientific, Waltham, MA, USA), Smart Orbit diamond ATR accessory (bench), Germanium slide-on ATR (microscope) and Spectra-Tech Micro Compression Cell with Diamond windows (Thermo Scientific, USA) were used on the cross-sections (samples MOM-A and MOM-B; Table 1). The cross-sections were analysed in micro-reflection and micro-ATR (Attenuated Total Reflectance) acquisition modes using an ATR objective of 20× with a Ge crystal and a pressure sensor in position 1. Infrared spectra were recorded in the region 4000–650 $cm^{-1}$, acquisition range with an MCT/A detector and micro-ATR (Si crystal), 64 scans for each spectrum, motorised stage, a spectral resolution of 4 $cm^{-1}$ and a mean spot size of 100 μm. Omnic 8.3 software was used for the management of the spectra.

### *2.9. Micro Raman Spectroscopy (μ-Raman)*

Micro Raman spectra were recorded both on cross-section MOM-A and micro samples MOM-E, MOM-F and MOM-G (Table 1) by a LabRAM HR-Evolution spectrometer (Horiba Jobin Yvon), employing 600 grooves per mm grating and a 200 μm confocal hole aperture (spectral resolution better than 7 $cm^{-1}$). The laser used was He–Ne with 633 nm wavelength emitting polarised light with a nominal maximum power of 17 mW. The spectrograph was coupled to an upright imaging microscope Olympus BXFM-ILHS with a 100× objective

enabling a spatial resolution of about 2 μm. Several points from each sample were randomly investigated without any preparation. Each measurement was recorded by adjusting the laser power by a nominal laser power lower than 1.7 mW at the microscope entrance, thus avoiding sample heating and spectrum distortion. A nonlinear baseline correction was applied.

## 3. Results

As a first step, the panel was submitted to X-radiography analysis to study the wood board structure, the location of the original batten system, now lost, and that of the joins. Digital microscope observations and image acquisition (magnification 50×–220×) of the panel surface allowed a first examination of the morphology and the technical features. Based on ED-XRF data, and by comparing the IRFC images with that of the reference pigments and dyes, the nature of the pigments in the different hues was assumed. Seven samples were subsequently collected and submitted to the different investigations (PLM, ESEM/EDX and ATR-FTIR) for assessing both the stratigraphic sequence and the compositional features, discriminating between original or not original matter. ATR-FTIR was also used to characterise the binders, even though this technique is not able to distinguish between protein sources [47]. Micro-Raman analysis carried out on four samples was used to integrate the other analyses.

### *3.1. Supports and Ground Preparation*

The panel support has a rectangular–vertical format (Figure 1a). Raking light observation of the back and lateral boards showed saw marks and a diagonal pattern due to the planer used for roughing. Other toolmarks, whose orientation is parallel to the direction of the wood fibres, are probably related to straight-pointed gouges, chisels and split blades used to complete the work.

From the XRR image, the support appears to be sufficiently homogeneous. It consists of three well-seasoned fir boards similar in size, arranged vertically and joined together along the direction of the fibres. Furthermore, the lateral boards were arranged in alternating positions to give stability to the panel. The original batten system, still visible on the back surface, is made of five horizontal crossbars. XRR showed the position of the riveted nails inserted from the *verso* to fix the crossbars.

Polarised light microscope (PLM) observations of the wood sample (MOM-H; Figure 1b) identified fir, whitish in colour, with evident growth rings and undifferentiated heartwood.

In some lacunae of the support, a double layer of linen cloth (*impannatura*) was observed (Figure 1c). As macro photographs and digital microscope observations indicated, the first layer is a lightweight linen canvas with a plain (1:1) weave, very close, characterised by a normal or Z-shaped twist of the yarn. The second one, separated from the previous one by a ground layer, has the same characteristics but is thicker and with a slightly open weave. ATR-FTIR spectrum of the linen fibres (Figure 2a) attested the presence of cellulosic compounds with absorption bands at 1160–1037 $cm^{-1}$, while the signals at 3291, 1659 and 1552 $cm^{-1}$, show peptide bonds of protein compounds [48]. Whewellite (Figure 2a) was also identified by its characteristic bands at 1315 and ~1650 $cm^{-1}$ ascribable to the $\nu_s$ (C-O) + δ(O-C=O) and $\nu_a$ (C=O) vibrational modes, respectively, and the pattern in the OH stretching vibrations (3600–3000 $cm^{-1}$) [49,50].

ED-XRF investigations carried out on white ground preparation revealed the occurrence of Ca, S, Sr, Si, Fe and K (Table S1) related to calcium sulphate as the main inorganic component of the ground. Silicate impurities and Sr-based minerals such as celestite ($SrSO_4$) were detected. PLM and ESEM/BSE investigations (Tables 2 and 3) of the cross-section samples (MOM-A and MOM-B) confirmed the presence of a coarse calcium sulphate ground layer (layer-1) having a thickness of more than 2 mm between two linen layers. The following ground layer is composed of five thin, homogeneous and smoothed levels. The presence of silicates, calcite, dolomite, kaolinite, microfossil and carbon black particles was identified in the ground layers (Tables 2 and 3; Figure S1).

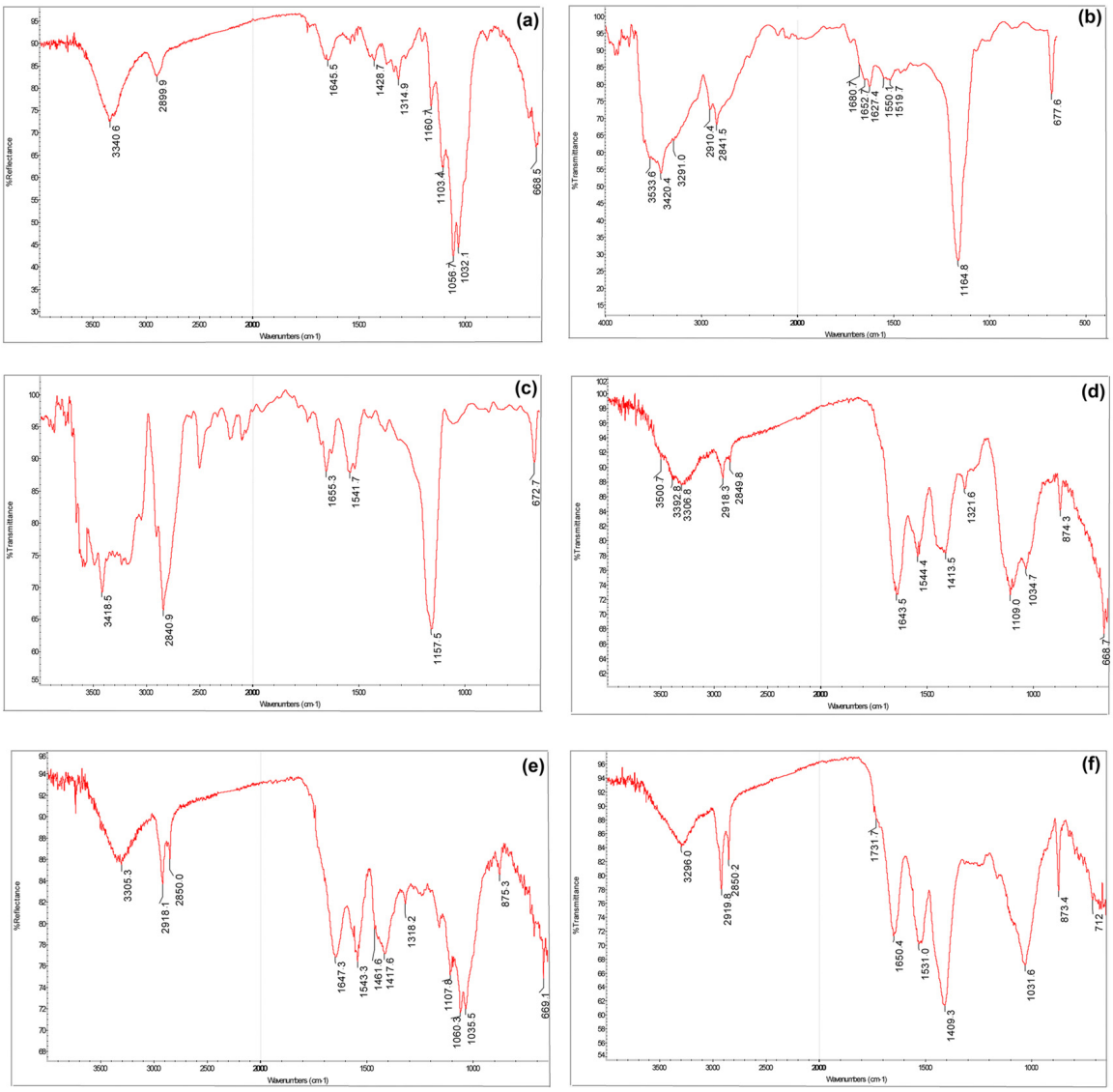


**Figure 2.** ATR-FTIR spectra: (**a**) linen fibre of sample MOM-B; (**b**) ground layer of sample MOM-A; (**c**) ground layer of sample MOM-B; (**d**) film-forming substance in sample MOM-B; (**e**) red lake glaze on the Sn-based foil in sample MOM-B; (**f**) painting layers, sample MOM-A.

**Table 2.** Sample MOM A description.

| Layer | Maximum Thickness (μm) | Typology | EDX, Detected Elements | Stratigraphic Identification (PLM, ESEM-EDX) | ATR-FTIR Identifications |
|---|---|---|---|---|---|
| 4 | 20 | repainting | C, Si, Al, Fe, K, Ca, Cu, P, Na, Ba, S | Fe-based pigments, Cu-based pigment, barite, organic matter | Proteins, silicates |
| 3 | 20 | | S, Hg, Si, Al, Fe, Mg, Ca | Mercury-based red, red ochre, calcium carbonate, bone black | |
| | | | C | Film-forming substance | |
| 2 | 20 | original paint layer | Al, Fe, Ca, Si, K, Na, Mg | Red ochre, haematite, calcium carbonate, quartz | Calcium carbonate, silicates, proteins, esters of carboxylic acids, lead carbonate |
| 1 | 55 | | Pb, C, Ca, P, Si, Al, K, Mg, Na | Minium, calcium carbonate, carbon black | |
| | | underdrawing | | | |

**Table 2.** *Cont.*

| Layer | Maximum Thickness (μm) | Typology | EDX, Detected Elements | Stratigraphic Identification (PLM, ESEM-EDX) | ATR-FTIR Identifications |
|---|---|---|---|---|---|
| 0 | 1250 | ground layer | S, Ca, Si, Mg, Na, Al, K, Fe, P | Calcium sulphate, silicates, calcite, dolomite, microfossil, carbon black | Calcium sulphate dihydrate, proteins |
| | | canvas | | Linen fibres | Cellulose, proteins |
| −1 | 1900 | ground layer | S, Ca, Fe, Si, Al, K, Na, Mg, P | Calcium sulphate, silicates, carbon black | Calcium sulphate dihydrate, proteins |
| | | canvas | | Linen fibres | Cellulose, calcium oxalates, proteins |

**Table 3.** Sample MOM-B description.

| Layers | Maximum Thickness (μm) | Typology | EDX, Detected Elements | Stratigraphic Identification (PLM, SEM/ESEM-EDX) | ATR-FTIR Identification |
|---|---|---|---|---|---|
| 5 | 10 | gilding | Au | Gold leaf | |
| 4 | 60 | bole | Pb, Si, Ca, Al, Mg, Fe, K, Na, Cl | Lead white, calcium carbonate, red ochre | Lead white, kaolinite, proteins, esters of carboxylic acids |
| 3 | 23 | underlayer | Ca, S | Calcium sulphate | Calcium sulphate dihydrate, lipidic compound, esters of carboxylic acids |
| 2 | 20–80 | paint | Sn, Al, Ca, Si, Fe, Mg, K, P | Red lake, tin mordant residues, red ochre | Anthraquinone compounds—red lake, calcium carbonate, calcium oxalates |
| 1 | 10 | gilding | C, Ag | Silver leaf, film-forming substance | Silicates, proteins, calcium carbonate, calcium oxalates |
| 0 | 1250 | ground layer | Ca, S, Si, Al, K, Fe, Mg, Cl, P, Na, Ti | Calcium sulphate, silicates, carbon black, linen fibres | Anhydrite, calcium sulphate dihydrate, proteins |
| | | canvas | | Linen fibres | Cellulose, calcium oxalates |
| −1 | 1600 | ground layer | Ca, S, Si, Al, K, Fe, Mg, Cl, P, Na, Ti | Calcium sulphate, calcium carbonate, kaolinite, silicates, microfossil | Anhydrite, proteins |

Calcium sulphate dihydrate ($CaSO_4 \cdot 2H_2O$) was detected in sample MOM-A (Figure 2b) due to the infrared bands at 3534, 3420, 1681, 1627, 1165 and 678 $cm^{-1}$ [31]. Conversely, anhydrite ($CaSO_4$) (Figure 2c) was found in the ground layer of sample MOM-B, showing stretching and bending absorptions of the $SO_4^{2-}$ groups, respectively, at ~1160 and 673 $cm^{-1}$. Traces of calcium sulphate dihydrate were also visible due to the two peaks at 1681 and 1624 $cm^{-1}$ [51].

Proteinaceous material (probable attributable to glue) was identified in the ground layers (Figure 2b) by specific absorbance values at 1650–1630 $cm^{-1}$ (amide I band), 1550–1520 $cm^{-1}$ (amide II) and the peak of N–H stretching at about 3000 $cm^{-1}$ [31,34]. The absorption bands in the fingerprint region of 1000–1450 $cm^{-1}$ could also be attributed to $CH_2$ wagging, $CH_3$ deformation, C-N and C-OH stretching of the proteinaceous material [51].

### *3.2. Preliminary Drawing*

IRFC identified the use of carbon-based black both in the underdrawing and in the outlining of the painting phase. Underdrawing and changes (*pentimenti*) were identified by IR reflectography (Figure S2a). The grey-black outlines were executed with a brush using a rather concentrated carbon-based black ink as per the response to multispectral analysis, which detected an intense absorption in the IR band. The drawing was not always visible under IR,

but it was clearer in the contour of the eyes and in the left hand of the Virgin, as well as on the left heel of the Child. The underdrawing appears coarse, uncertain and inaccurate as a broad and rapid brushstroke was used. A clear example is provided by traces near the shoulder of the Virgin in which a line appears deviated from the image construction, overlapping the correct one that should have been its continuation (Figure S3a).

In several cases, therefore, the drawing is not faithful and precise compared to the final painting, and they do not match together. In this sense, the figure of the Child examined through IR reflectography is worthy of attention; below the reddish-brown mantle, a series of folds of the drapery are not perceivable in the pictorial phase. This sort of *sottomodello* emerged in correspondence with the left sleeve or above the Child's right ankle [52].

Carbon black was detected by μ-Raman in the sample collected from the underdrawing (MOM-G) due to a broad and strong band at about ~1580 $cm^{-1}$ as a result of defects of the graphite structure or disorder band (D band) and a weaker one at~1324 $cm^{-1}$ (Figure S3b) attributed to stretching vibrations in the planar graphite structure (G band) ([50] and references therein, [53]).

### *3.3. Decoration and Gilding*

Haloes of the Virgin and Child, eight-pointed stars, fibula and hem of the mantle are free-hand-decorated in relief, probably shaped using gypsum (*pastiglia* technique), as the high signals of C and S confirm. In the gilding areas of the Child's halo and the background, ED-XRF analyses allowed us to detect Ag and Au (Table S1). Cu was identified only in the dark contour lines of the Child's halo, and it could be related to gold impurity [29]. Hg and S are attributable to the Hg-based red pigment used to outline the red cross profile.

In sample MOM-C, collected from the background (Figure 1a), ESEM morphological observations and EDX microanalysis revealed the presence of the original Ag-based leaf, although discontinuous (Figure S4a,b). Ca and S are related to the ground, and minor amounts of Si, Al, Mg, Fe and Na are associated with Fe-rich clayey pigments, which were commonly used with metal-leaf adhesives [29]. Cl occurrence should be ascribable to degradation products [29].

PLM observations, ESEM-EDX analysis and elemental map carried out on the MOM-B cross-section confirmed the presence of a first discontinuous thin Ag-based leaf and a yellowish fluorescence (Figures 3a,b,g and S5a–c; Table 3).

ATR-FTIR spectrum (Figure 2d) detected the presence of proteins, probably glue (~3300, 1643, 1544 $cm^{-1}$), calcium carbonate (1414, 874 $cm^{-1}$), calcium oxalates, mostly weddellite (1322 $cm^{-1}$) and silicates (1109–1034 $cm^{-1}$) [31]. Superimposed on the original Ag foil, a red lake-based layer was found due to the presence of anthraquinone compounds (1647, 1543, 1461 $cm^{-1}$; Figure 2e). Sn particles (Figure 3a,b,h), varying in sizes and morphologies, were detected by ESEM/EDX, suggesting the use of red dyestuff stabilised by tin oxides ($SnO_2$) [54]. Calcium carbonate ($CaCO_3$) (1410–1413, 875 $cm^{-1}$), calcium oxalates and whewellite (1318 $cm^{-1}$) were detected by ATR-FTIR due to the band at 1318 $cm^{-1}$ [31]. A layer composed of calcium sulphate dihydrate and esters of carboxylic acids (2929, 1725, 1730–1710 $cm^{-1}$) was also detected [31]. The overlying layer is made of lead white (1399, 681 $cm^{-1}$) and kaolinite (~1100–911 $cm^{-1}$); the peaks at 1640 and 1544 $cm^{-1}$ demonstrate the presence of proteinaceous material, and the peaks at 2929 and 1725 $cm^{-1}$ (esters of carboxylic acids) could suggest the use of drying oil and/or fatty components [31,34]. The final, not original, gilding is composed of an Au-based leaf (Figures 3b,j and S5d).

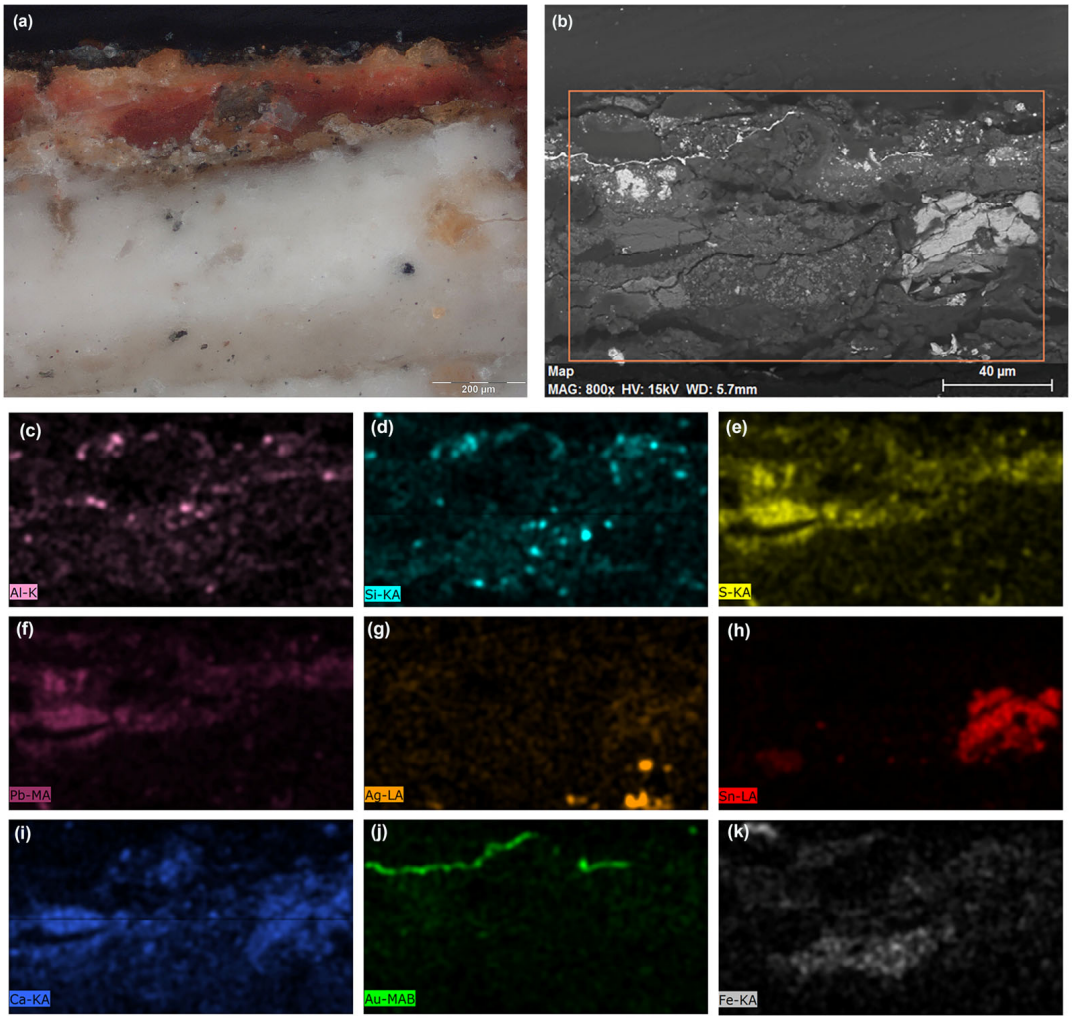


**Figure 3.** Micrographs of sample MOM-B cross-section: (**a**) PLM detail of the painting layers in reflected light; (**b**) ESEM-BSE with the EDX elemental distribution map area; EDX element distribution of (**c**) Al; (**d**) Si; (**e**) S; (**f**) Pb; (**g**) Ag; (**h**) Sn; (**i**) Ca distribution; (**j**) Au distribution; (**k**) Fe distribution.

### *3.4. Painting Materials*

High levels of Pb, Hg and S were detected by ED-XRF in the red hues (Table S1; Figure 1). IRFC (Figure S2b) confirmed the massive use of Pb-based red, probably preferable to minium ($Pb_3O_4$) and mercury-based red (cinnabar/vermilion) [55], which gives the drapery a suggestive red-orange shade, such as in the Virgin's red garment (MO6,7) and Child's robe (MO8). The use of mercury-based red (HgS) is evident in the globular fibula of Christ, along the profile of Christ's head and over his foot, in the centre of the space between Christ's forehead and the top of the nimbus, on the scroll in the Child's hands, above the eyes of both figures, in trace on the jewel on the Virgin's chest and in her upper lip.

Red contour lines of anatomical details are executed by mixing mercury-based red with Fe-based pigments (MO12). Sometimes Cu-based pigment was also used to create shady areas, such as in Virgin's eyebrow or lip (MO13,16) and in the child's halo outline (MO18a). In the brown hues, the presence of Fe, Si and K are related to red and brown ochre. Traces of Mn and P could be related to Mn-oxides and bone black ($Ca_3(PO_4)_2$). According to OM and ED-XRF results (Table S1; Figure 1a), the Virgin's flesh (MO1-3,11,13,14,15) and lip (MO16) are presumably made of a mixture of lead white ($2PbCO_3 \cdot Pb(OH)_2$), mercury-based red and Fe-based pigments (red ochres). The different hues (light and shadow) show

slight variations in the content of Pb-white, Fe-based pigments (ochres), bone black and Mn oxides.

According to micro-invasive analyses, sample MOM-A, collected in the red *maphorion* of the Virgin (Table 1), showed a very complex stratigraphy (Figures 4a–i and S6a; Table 2) and weak yellowish fluorescence (Figure S6b). The first layer is composed of red Pb-based particles, related to minium, bone-black particles, calcium carbonate and silicate—proved by the presence of Si, Al, K, Fe, Ca, Na and P. The second layer was obtained using red ochre-rich and bone-black particles. A film-forming substance is present between the sub-mentioned painting layers and the other two overlaid repainting layers (Table 2), the first of which is composed of mercury-based red, red ochre, calcium carbonate and bone black, whose presence is confirmed by ESEM-EDX. Fe-based pigments, Cu-based pigments and Ba-sulphate were identified in the second layer [56].

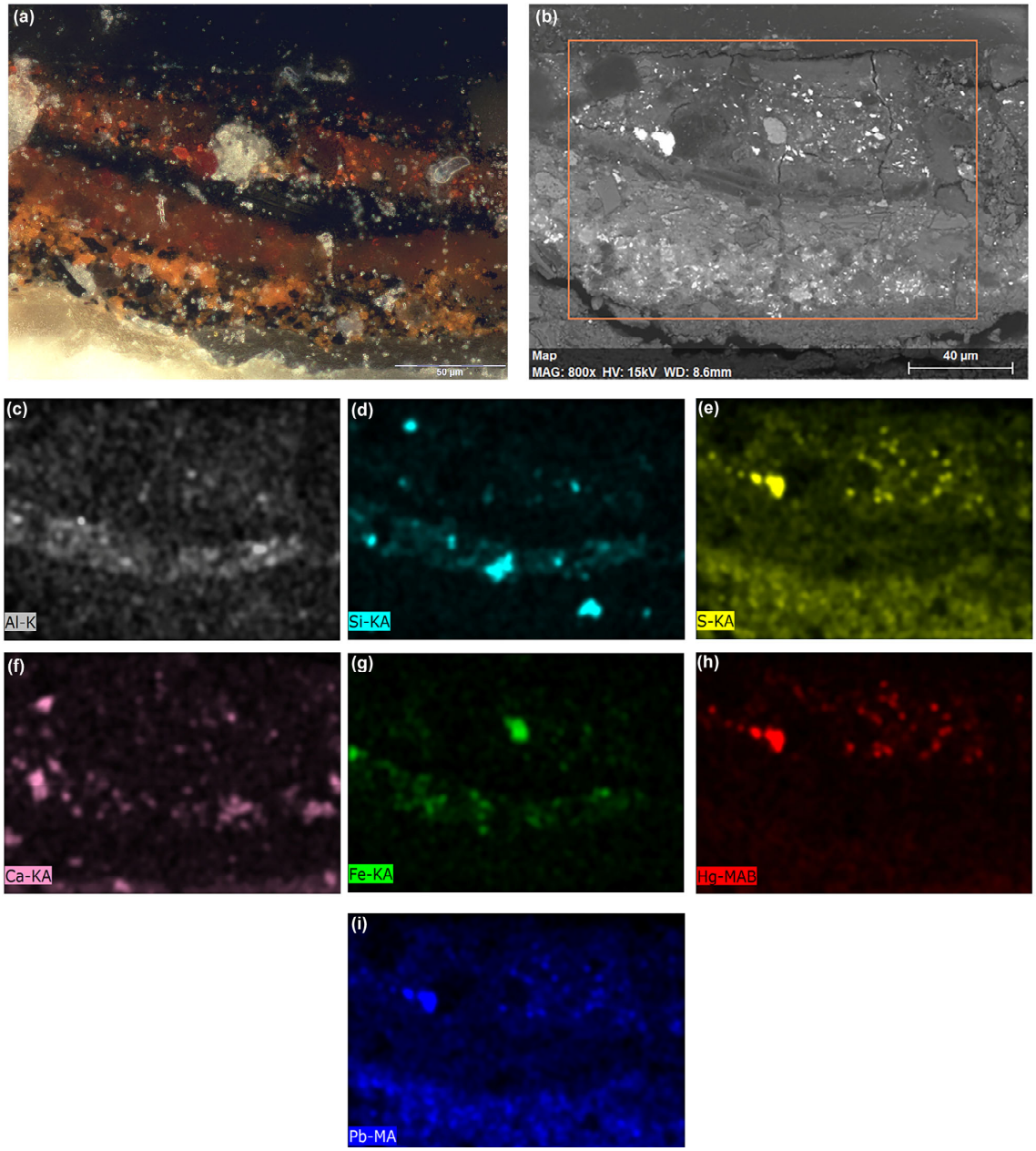


**Figure 4.** Micrographs of sample MOM-A cross-section: (**a**) PLM detail of the painting layers in reflected light; (**b**) ESEM-BSE micrograph with EDX elemental distribution map; EDX element distribution of (**c**) Al; (**d**) Si; (**e**) S; (**f**) Ca; (**g**) Fe; (**h**) Hg; (**i**) Pb.

μ-Raman analysis carried out on sample MOM-A detected haematite and calcite (Figure 5a,b) respectively due to the bands at 219, 290, 405, 495, 605, 1306 $cm^{-1}$ [50] and 153, 280, 717, 1086 $cm^{-1}$ [57].

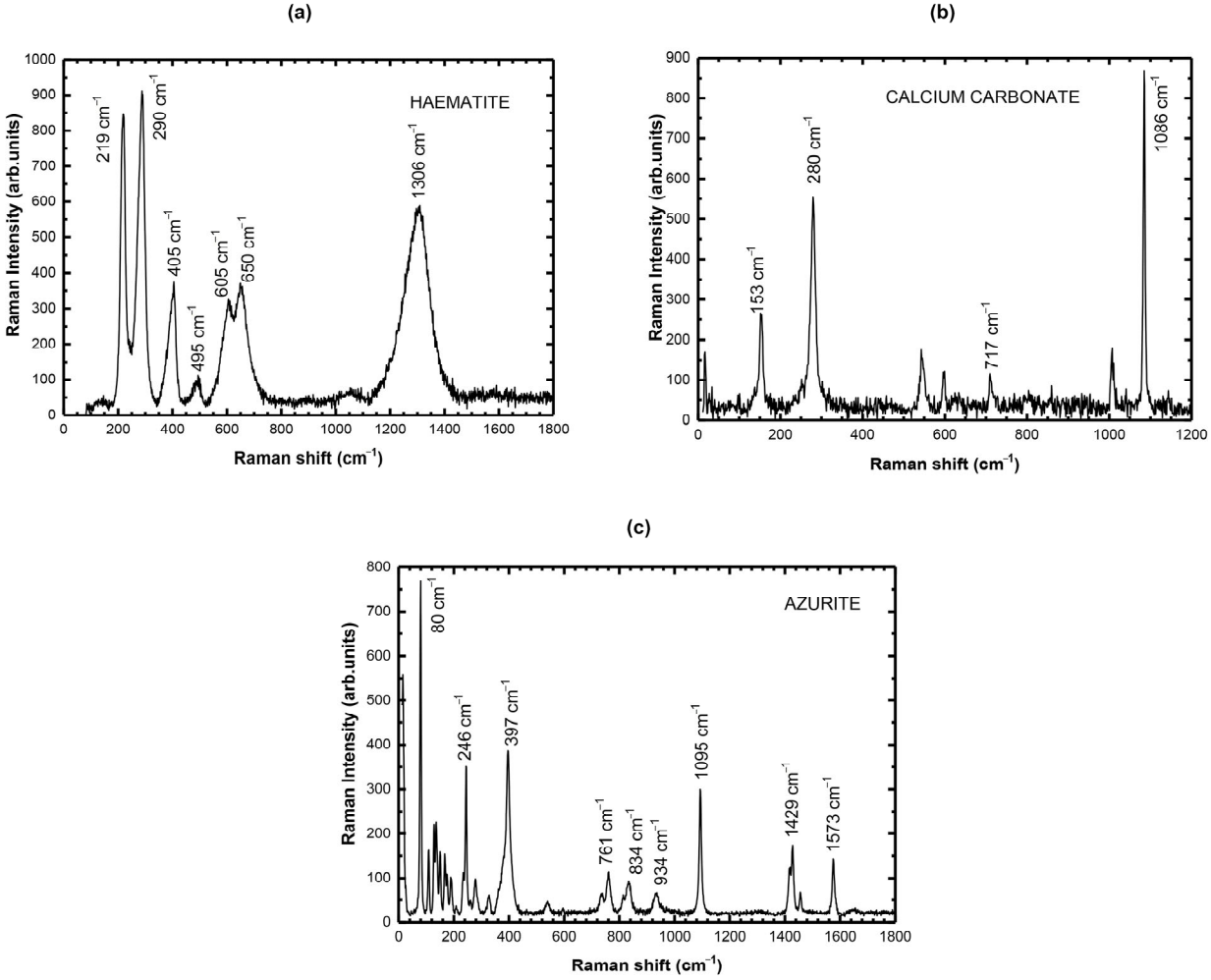


**Figure 5.** Raman spectra of sample MOM-A: (**a**) haematite and (**b**) calcium carbonate; sample MOM-E: (**c**) azurite.

ATR-FTIR analysis (Figure 2f; Table 2) carried out on the first two layers of sample MOM-A confirms the use of a proteinaceous medium, presumably egg yolk, due to the typical protein bands: CHstr (2920, 2850 $cm^{-1}$), C=O stretching (1730–1710 $cm^{-1}$), amides I and II (1650–1530 $cm^{-1}$) [33,58]. The presence of lead carbonates in the red lead-based layer should be assumed due to distinctive peaks at 1409 and ~680 $cm^{-1}$ [59]. Signals related to calcite (1409, 873, 712 $cm^{-1}$), silicates (~1100–900 $cm^{-1}$) and proteins (3286, 1646, 1539 $cm^{-1}$) were also detected in the last two repainting layers (Table 2).

ED-XRF investigations of the blue Virgin's dress (MO 4,17; Table S1, Figure 1a) detected the presence of lead white and Cu-based pigments that IRFC indicated to be azurite ($Cu_3(CO_3)_2(OH)_2$) (Figure S2b). The presence of azurite, a basic copper (II) carbonate, in sample MOM-E (blue Virgin's sleeve) was demonstrated by its characteristic Raman peaks at 80, 246, 397,761, 834, 1095, 1429, 1575 $cm^{-1}$ (Figure 5c) [58].

### *3.5. Previous Restoration*

Due to the different fluorescence, UV images highlighted plastering and pictorial retouches related to the different restoration interventions, especially in the vertical direction between the junction of the wooden boards (Figure S1b). The bluish fluorescence could be related to an unoriginal synthetic varnish, such as the one applied on the Virgin's dress.

UV fluorescence gives a faded response when the unoriginal varnish was applied above the repainting, while it appears black when the retouches were applied on the varnish layer [60].

The oldest intervention on the Virgin *Hodegetria* panel, dating back after 1427 [3], consisted of the introduction of the two angels at the upper corners (Figure 1a), directly painted on the silver background. In 1811, probably following the firing of the Cathedral, the panel underwent a dramatic aesthetic change, which involved an almost total repainting of the surface. Due to the conviction that the original technique involved a gold background or simply responding to new aesthetic requirements, the original silver leaf was probably scratched and covered by applying a gold leaf. As shown by the historical images of the Virgin's mantle (Figure S2c), four eight-pointed stars have been painted, readjusting the two originals according to the new relief style. Similarly, the hem of the Virgin's mantle and the floral decorations on her left shoulder were repainted and regilded.

The former intervention, dating back to 1960, is documented by old photos. During that intervention, the original crossbeams were substituted with a new batten system, consisting of three mobile horizontal crossbars made of a coniferous tree. The 19th-century repainting was removed mechanically, as shown by the numerous signs of metal blades visible on the surface in raking light, and new pictorial reintegration was applied.

Due to the intense pink-fuchsia IRFC false chroma on the background in Christ's sleeve and in the lower veil of the Virgin, indigo presence was related to the repainting intervention. Other blue pigments, such as smalt blue, also occurred due to the intense reddish IRFC response (Figure S2b). The greenish nuance in the IRFC image is compatible with the presence of red ochres, even if they are brownish in visible light [61].

Micro-Raman carried out on the sample MOM-F (blue-red traces on the background) confirmed the presence of indigo, due to the bands at 249, 544, 597, 1575 $cm^{-1}$. Orpiment, due to the bands at 154, 200, 294, 309, 353, 384 $cm^{-1}$ [57], and synthetic Mars, for the signals at 220, 290, 401, 410, 660 $cm^{-1}$ [53], were also detected. In the MOM-D sample (blue traces on the background; Figure S7a), ESEM/EDX detected Si, Pb, K, Ca, Fe, As, Al, Na and Co related to Fe-based pigments and smalt blue (Figure S7b).

## 4. Discussion

The Virgin *Hodegetria* panel still keeps its original frame composed of four wooden rulers fixed by riveted nails; this is a common type of frame used in Mediterranean icons and medieval panels [62] that differs from the traditional Byzantine technique because of the icons that are unframed [63].

The choice of sub-radial cut boards, which are less subject to deformations and dimensional variations, denotes accuracy in the execution of the panel [64]. According to the small size of the collected wood sample, an unquestionable identification among the different species of *Abies* by anatomical wood features is difficult [65]. The genus Abies is widespread in the Mediterranean basin and is frequently used in earlier supports of central and northern Italian paintings [66]. The use of *Abies* sp. is attested in the decorative elements of the wooden ceiling of the Palatine Chapel in Palermo (XII century) [67].

The presence of linen canvas (*impannatura*) quite distant from the junctions of the boards indicates that cloth covered the entire front surface of the panel, as one might expect from a painting dating back to the first half of the 12th century [21].

Gypsum, anhydrite and a glue-based binder were detected in the ground layers, mixed with clay, silicates, calcite, and carbon black, as mentioned in the literature [31,36,68–70]. According to Gomez et al., celestite presence is associated with gypsum deposits in sedimentary rocks [71].

Carbon black was used for the underdrawing. The drafting of a graphic outline (*graphià*) to follow in the subsequent pictorial phase was essential in the medieval technique, and especially in the production of the painted icons, in which the drawing was indicated as one of the canonical steps of the executive process.

In the Hodigitria panel, the essentiality of the decor and the presence of limited gypsum-based reliefs recall a consolidated procedure used both in Southern Italy and in the Byzantine world [8,63]. According to the results, an Ag-based original leaf was detected. Confirmation of silvery use is provided by Bartholomeus Angelicus in the 13th century *De Proprietatibus Rerum* treatise [72] and by Theophilus [21]. Silver background and relief-gesso halo with floral patterns are features commonly found in Cyprus icons from the 13th century [11] but rarely found elsewhere [10]. No bole preparation was found under the silver leaf, and a mission technique was supposed due to the presence of a film-forming substance that was probably applied to receive the Ag-gilding. According to the literature, the appearance of the bolus was attested in the 15th century but widespread in the 16th century [41,73]. The original Ag leaf of the frame was covered with a red tin-complexed lake and later regilded with Au leaf. The presence of red dyestuff stabilised by tin oxides (SnO2) in the panel frame, between Ag and Au gilding, is very interesting and confirmed a late restoration intervention, as this type of red lake was available between the end of the 18th century and the beginning of the 19th century [54]. The Au-based leaf was applied after this date and then removed during the 1960s–1970s intervention, but traces of this regilding remain on both the bottom and the halos.

The original pigments used are red lead, red ochre, azurite, carbon black and bone black with a proteinaceous binder, according to the Italian painting tradition of the 13–14th centuries [21]. Mercury-based red, indigo, smalt blue, lead white, orpiment, synthetic Mars and oil binder are probably related to the different restoration interventions that occurred over the centuries.

## 5. Conclusions

According to its size, the Virgin Hodigitria panel is oversized to be an icon by comparing with other local depictions of rectangular format and similar subjects in which the Virgin has been represented by half-length. Anyway, southern Italian influences and Byzantine iconographic elements of the 13th century still persist in the panel both in the iconographic apparatus and in the technical representation of the colours and anatomical details [74].

Concerning the executive technique, the composition of the ground layer agrees with the Italian painting tradition described by Theophilus, and it is also confirmed by the presence of linen between the wood support and the ground layer.

The occurrence of dark grey accurate lines in the carbon-based underdrawing suggested the use of a brush. The underdrawing was essential in medieval technique, and especially in the production of painted icons, in which the drawing was considered one of the canonical steps of the executive process [52].

Thanks to the investigations, the original silver leaf was detected in the background and haloes of the Virgin and Child. Over time, a misunderstanding of the original gilding caused the application of both a red lake on the silver background to imitate the gilding effect and, later, a gold leaf.

The *Hodegetria* panel was originally painted with a proteinaceous binder, probably egg tempera, using red ochre, hematite, red lead, carbon black, bone black and azurite. The non-original pigments used in the several restoration interventions are mercury-based red, indigo, blue smalt, lead white, orpiment and synthetic Mars red. Synthetic varnishes were also applied during the most recent restoration interventions.

The restoration of the *Hodegetria* panel was more than a simple opportunity to recover an object of unquestionable cultural value, as it represented the possibility of improving the knowledge of 13th-century southern paintings.

**Supplementary Materials:** The following supporting information can be downloaded at: https://www.mdpi.com/article/10.3390/heritage6060249/s1, Figure S1. Sample MOM-A: (a) PLM micrograph of the ground layer in reflected light; (b) ESEM/BSE micrograph of the microfossil in the ground layer; Figure S2. The Virgin *Hodegetria* panel painting: (a) IR reflectography; (b) IRFC image; (c) historical photo after the restoration carried out in the 19th century; (d) after the recent restoration intervention;

Figure S3. (a) Underdrawing traces in the lacuna of Virgin's shoulder; (b) sample MOM-G: μ-Raman spectrum of carbon black; Figure S4. (a) Macro photograph of silver leaf traces on the background; (b) sample MOM-C: ESEM/EDX spectrum of the original silver leaf; Figure S5. Sample MOM-B: (a) PLM micrograph, UV light; (b) ESEM/EDX micrograph, detail of the original Ag leaf on the ground layer; (c) EDX spectrum of Ag leaf; (d) EDX spectrum of Au leaf; Figure S6. Sample MOM-A: (a) PLM micrograph, detail of painting layers; (b) PLM micrograph, UV light; (c) ESEM/EDX micrograph, microanalysis detail; (d) EDX spectrum of red lead-based layer; Figure S7. (a) Blue traces of repainting layer, upper left corner, detail; (b) sample MOM-D: ESEM/EDX spectrum of the repainting layer; Table S1: ED-XRF analysis measurement point (ED-XRF/MP), description and elemental composition of the investigated areas.

**Author Contributions:** Conceptualization, M.L.A. and M.S.; Data curation, M.L.A. and V.M.; Formal analysis, M.L.A., C.P., S.A. and V.M. Funding acquisition, B.P., M.L.A.; Investigation, M.L.A., V.M., C.P., S.A. and B.P; Multispectral investigation, P.T.; Methodology, M.L.A., C.P.; Project administration, M.L.A. and M.S.; Resources, M.S.; Supervision, M.L.A. and V.M.; Validation, M.L.A. and C.P.; Writing—original draft, M.L.A., M.S. and C.P.; Writing—review & editing, M.L.A. and V.M. All authors have read and agreed to the published version of the manuscript.

**Funding:** This work was supported by PON03PE_00214_1 Nanotecnologie e nanomateriali per i beni culturali (TECLA PROJECT) and Project_DISPEA, University of Urbino, CUP H31I18000020005.

**Acknowledgments:** We wish to thank: Salerno G., Diagnostic Medical Centre Pa.ma.fi.r. Palermo, for X-Radiography; Amato F. and Miccichè C. for support in the Micro Raman measurements; Macchioni N. for wooden species identification; Frezzato F. and Monni E. for ATR-FTIR support; Lavrentev V. and Korsunova D. for English editing.

**Conflicts of Interest:** The authors declare no conflict of interest. The funders had no role in the design of the study; in the collection, analyses, or interpretation of data; in the writing of the manuscript; or in the decision to publish the results.

## References

1. Travagliato, G. La Madonna della Bruna di Monreale: Un testimone della maniera cypria nell'abbazia benedettina del re Guglielmo II. In *L'Odigitria detta "di Guglielmo II" della Cattedrale di Monreale*; Sebastianelli, M., Travagliato, G., Eds.; Palermo University Press: Palermo, Italy, 2019; pp. 18–41.
2. Di Natale, M.C. Criteri di Museologia per il Museo Diocesano di Monreale. *OADI* **2015**, *12*, 15–16.
3. Di Natale, M.C. L'icona di Monreale. In *L'Odigitria detta "di Guglielmo II" della Cattedrale di Monreale*; Sebastianelli, M., Travagliato, G., Eds.; Palermo University Press: Palermo, Italy, 2019; pp. 13–16.
4. Travagliato, G. Icona graece, latine Imago dicitur: Culture figurative a confronto in Sicilia (secc. XII-XIX). In *Tracce d'Oriente. La Tradizione Liturgica Greco-Albanese e Quella Latina in Sicilia, Catalogo Della Mostra (Palermo, Palazzo Bonocore, 26 Ottobre–25 Novembre 2007)*; Di Natale, M.C., Ed.; Edizioni Plaza Fondazione: Palermo, Italy, 2007; pp. 42–43.
5. Chatzidakis, N. A Byzantine icon of the dexiokratousa Hodegetria from Crete at the Benaki Museum. In *Images of the Mother of God, Perceptions of the Theotokos in Byzantium*; Vassilaki, M., Ed.; Ashgate Publishing: Aldershot Hampshire, UK, 2005; pp. 337–406.
6. Papageorghiou, A. *Icons of Cyprus*; Holy Archbishop of Cyprus: Nicosia, Cyprus, 1992; pp. 16–21.
7. Sophocleus, S. Le peintre Theodoros Apsevidis et son entourage, Chypre 1183 et 1192. In *Byzantinische Malerei. Bildprogramme-Ikonographie-Stil*; Dr Ludwig Reichert Verlag: Wiesbaden, Germany, 2000; p. 319.
8. Pace, V. La Puglia fra arte bizantina e maniera greca. In *Ars auro gemmisque prior. Mélanges en hommage à Jean-Pierre Caillet*; Blondeau, C., Boissavit-Camus, B., Boucherat, V., Volti, P., Eds.; University of Zagreb: Zagreb, Croatia, 2013; pp. 491–498.
9. Frinta, M.S. Raised gilded adornment of the Cypriot icons, and occurrence of the technique in the west. *Gesta* **1981**, *20*, 333–347. [CrossRef]
10. Mouriki, D. A Thirteen-Century Icon with a variant of the Hodegetria in Byzantine Museum of Athens. In *Dumbarton Oaks Papers, Studies on Art and Archeology in Honor of ErnstKitzinger on His Seventy-Fifth Birthday*; Dumbarton Oaks: Washington, WA, USA, 1987; Volume 41, pp. 403–414. [CrossRef]
11. Sebastianelli, M. La Madonna Odigitria del Duomo di Monreale dalla leggenda alla realtà: Storia, tecnica e restauro critico di un'antica icona. In *L'Odigitria detta "di Guglielmo II" della Cattedrale di Monreale*; Sebastianelli, M., Travagliato, G., Eds.; Palermo University Press: Palermo, Italy, 2019; pp. 55–131.
12. Pellerito, C.; Sebastianelli, M.; Raineri, R.; Megna, B.; Di Natale, M.C.; Pignataro, B.; Amadori, M.L.; Palla, F. Le indagini scientifiche per lo studio e la conservazione dei beni culturali: Un approccio analitico integrato, la conoscenza dei materiali costituitivi e della tecnica esecutiva della Madonna Odigitria di Monreale. In *L'Odigitria detta "di Guglielmo II" della Cattedrale di Monreale*; Sebastianelli, M., Travagliato, G., Eds.; Palermo University Press: Palermo, Italy, 2019; pp. 133–142.

13. Weitzmann, K. Crusader icons and "La Maniera Greca"—Le Icone crociate e la "maniera greca". In *Il Medio Oriente e l'Occidente*; Belting, H., Ed.; Atti del 24° Congresso Internazionale CIHA (Bologna 1979): Bologna, Italy, 1982; pp. 71–77.
14. Belting, H. *Likeness and Presence: A History of the Image before the Era of Art*; University of Chicago Press: Chicago, IL, USA, 1994; pp. 4–5.
15. Demus, O. *L'arte Bizantina e l'Occidente*; Einaudi: Torino, Italy, 2008.
16. Bacci, M. San Luca: Il pittore dei pittori. In *Artifex Bonus. Il Mondo Dell'artista Medievale*; Castelnuovo, E., Ed.; Laterza: Bari, Italy, 2004; pp. 3–11.
17. Lidov, A. *The Miraculous Image in the Late Middle Ages and Renaissance*; L'erma Di Bretschneider: Rome, Italy, 2004; pp. 273–304.
18. Vasari, G. De la pittura. In *Le vite de' più eccellenti pittori, scultori, e architettori, Firenze 1550 (Torrentino) e 1568 (Giunti)*; Bellosi, L., Rossi, A., Eds.; Einaudi: Torino, Italy, 1991; Volume I, p. 66.
19. Schmidt, V.M. Tavole dipinte. Tipologie, destinazioni e funzioni (secoli XII-XIV). In *L'arte Medievale nel Contesto*; Piva, P., Ed.; Jaka Book: Milano, Italy, 2006; pp. 211–212.
20. Sandberg Vavalà, E. *L'iconografia della Madonna col Bambino nella Pittura Italiana del Dugento*; Multigrafica Editrice: Roma, Italy, 1983; p. 38.
21. Teofilo. Translation and References by Tantalo, A. In *Sulle Diverse Arti*; Grandieri, M., Ed.; B.A. Graphics: Milano, Italy, 2005; pp. 18–19, 22–23.
22. Thompson, D.V. *The Materials and Techniques of Medieval Painting*; Dover Publications: New York, NY, USA, 1956; pp. 105–117.
23. Marette, J. *Connaissance des Primitifs par l'étude du Bois, du XIIe au XVIe Siècle*; A. & J. Picard: Paris, France, 1961; p. 285.
24. Bomford, D.; Kirby, J. *Art in the Making: Italian Painting before 1400: National Gallery London, 29 November 1989–28 February 1990*; National Gallery: London, UK, 1990.
25. Bellucci, R.; Castelli, C.; Ciani Passeri, F.; Ciatti, M.; Giovannini, C.; Parri, M.; Petrone, P.; Rossi Scarzanella, C.; Santacesaria, A. Tecniche pittoriche del XIII secolo: Il dossale di Meliore di Jacopo in San Leolino a Panzano. *OPD Restauro* **1990**, *2*, 186–211.
26. Ramos-Poquí, G. *The Technique of Icon Painting*; Burns & Oates/Search Press: Tunbridge Wells, UK, 1999.
27. Weissmann, G. *Techniques of Traditional Icon Painting*; Since Press LTD: Tunbridge Wells, UK, 2012.
28. Ciatti, M. Some observations on panel painting technique in Tuscany from the twelfth to the thirteenth century. *Stud. Conserv.* **2013**, *43*, 1–4. [CrossRef]
29. Mastrotheodoros, G.P.; Beltsios, K.G.; Bassiakos, Y.; Papadopoulou, V. On the metal-leaf decorations of post- Byzantine Greek icons. *Archaeometry* **2018**, *60*, 269–289. [CrossRef]
30. Sotiropoulou, S.; Daniilia, S. Material aspect of icons. A review on physiochemical study of Greek icons. *Acc. Chem. Res.* **2010**, *43*, 877–887. [CrossRef]
31. Lazidou, D.; Lampakis, D.; Karapanagiotis, I.; Panayiotou, C. Investigation of cross-section stratifications of icons using micro-Raman and micro-Fourier Transform Infrared (FT-IR) Spectroscopy. *Appl. Spectrosc.* **2018**, *72*, 1258–1271. [CrossRef]
32. Daveri, A.; Doherty, B.; Moretti, P.; Grazia, C.; Romani, A.; Fiorin, E.; Brunetti, B.G.; Vagnini, M. An uncovered XIII century icon: Particular use of organic pigments and gilding techniques highlighted by analytical methods. *Spectrochim Acta A Mol.* **2015**, *135*, 398–404. [CrossRef]
33. Salvadó, N.; Pradell, T.; Pantos, E.; Papiz, M.Z.; Molera, J.; Seco, M.; Vendrell-Saz, M. Identification of copper-based green pigments in Jaume Huguet's Gothic altarpieces by Fourier transform infrared microspectroscopy and synchrotron radiation X-ray diffraction. *J. Synchrotron Radiat.* **2002**, *9*, 215–222. [CrossRef]
34. Sandu, I.C.A.; Bracci, S.; Sandu, I.; Lobefaro, M. Integrated Analytical Study for the authentication of five Russian Icons (16th–17th centuries). *Microsc. Res. Tech.* **2009**, *72*, 755–765. [CrossRef]
35. Miguel, C.; Lopes, J.A.; Clarke, M.; Melo, M.J. Combining infrared spectroscopy with chemometric analysis for the characterization of proteinaceous binders in medieval paints. *Chemom. Intell. Lab. Syst.* **2012**, *19*, 32–38. [CrossRef]
36. Platania, E.; Streeton, N.L.W.; Lluveras-Tenorio, A.; Vila, A.; Buti, D.; Caruso, F.; Kutzke, H.; Karlsson, A.; Colombini, M.P.; Uggerud, E. Identification of green pigments and binders in late medieval painted wings from Norwegian churches. *Microchem. J.* **2020**, *156*, 104811. [CrossRef]
37. Franceschi, E.; Nole, D.; Vassallo, S. Archaeometric Non-Invasive Study of a Byzantine Albanian Icon. *J. Sci. Res. Rep.* **2013**, *2*, 17–34. [CrossRef]
38. Daniilia, S.; Bikiaris, D.; Burgio, L.; Gavala, P.; Clark, R.J.H.; Chryssoulakis, Y. An extensive non-destructive and micro-spectroscopic study of two post-Byzantine over-painted icons of the 16th century. *J. Raman Spectrosc.* **2002**, *33*, 807–814. [CrossRef]
39. Karapanagiotis, I.; Minopoulou, E.; Valianou, L.; Daniilia, S.; Chryssoulakis, Y. Investigation of the colourants used in icons of the Cretan School of iconography. *Anal. Chim. Acta* **2009**, *647*, 231–242. [CrossRef]
40. Valianou, L.; Wei, S.; Mubarak, M.S.; Farmakalidis, H.; Rosenberg, E.; Stassinopoulos, S.; Karapanagiotis, I. Identification of organic materials in icons of the Cretan School of iconography. *J. Archeol. Sci.* **2011**, *38*, 246–254. [CrossRef]
41. Armetta, F.; Chirco, G.; Ciaramitaro, V.; Caponetti, E.; Midiri, M.; Saladino, M.L. Sicilian Byzantine Icons through the Use of Non-Invasive Imaging Techniques and Optical Spectroscopy: The Case of the Madonna dell'Elemosina. *Molecules* **2021**, *26*, 7595. [CrossRef]
42. Sandu, I.C.A.; Afonso, L.U.; Murta, E.; De Sa, M.H. Gilding techniques in religious art between East and West, 14th–18th centuries. *Int. J. Conserv. Sci.* **2010**, *1*, 47–62.

43. Conover, D.M.; Delaney, J.K.; Loew, M.H. Automatic Registration and Mosaicking of Conservation Images. In *Optics for Arts, Architecture, and Archaeology IV*; SPIE: Bellingham, WA, USA, 2013; Volume 87900A. [CrossRef]
44. Dyer, J.; Verri, G.; Cupitt, J. *Multispectral Imaging in Reflectance and Photo-Induced Luminescence Modes: A User Manual*; Online: European CHARISMA Project; The British Museum: London, UK, 2013; pp. 122–151.
45. Triolo, P.A.M. *Manuale Pratico di Documentazione e Diagnostica per Immagine per i BB.CC*; Il Prato: Saonara, Italy, 2019; pp. 222–223.
46. Cartwright, C.R. The principles, procedures and pitfalls in identifying archaeological and historical wood samples. *Ann. Bot.* **2015**, *116*, 1–13. [CrossRef]
47. Mazzeo, R.; Menu, M.; Amadori, M.L.; Bonacini, I.; Itié, E.; Eveno, M.; Joseph, E.; Lambert, E.; Laval, E.; Prati, S. Examination of the Uomini Illustri: Looking for the Origins of the portraits in the Studiolo of the Ducal Palace of Urbino. Part 2. In *Studying Old Master Paintings: Technology and Practice*; Spring, M., Ed.; Archetype Publications and the National Gallery: London, UK, 2011; pp. 44–51.
48. Pellegrini, D.; Duce, C.; Bonaduce, I.; Biagi, S.; Ghezzi, L.; Colombini, M.P.; Tinè, M.R.; Bramanti, E. Fourier Transform Infrared Spectroscopic Study of Rabbit Glue/Inorganic Pigments Mixtures in Fresh and Aged Reference Paint Reconstructions. *Microchem. J.* **2015**, *124*, 31–32. [CrossRef]
49. Conti, C.; Casati, M.; Colombo, C.; Realini, M.; Brambilla, L.; Zerbo, G. Phase transformation of calcium oxalate dihydrate–monohydrate: Effects of relative humidity and new spectroscopic data. *Spectrochim. Acta A Mol. Biomol. Spectrosc.* **2014**, *128*, 413–419. [CrossRef] [PubMed]
50. Amadori, M.L.; Mengacci, V.; Vagnini, M.; Casoli, A.; Holakooei, P.; Eftekhari, N.; Kyi, L.; Maekawa, Y.; Germinario, G. Organic Matter and Pigments in the wall Paintings of Me-Taw-Ya Temple in Bagan Valley, Myanmar. *Appl. Sci.* **2021**, *11*, 11441. [CrossRef]
51. Lane, M.D. Mid-infrared emission spectroscopy of sulphate and sulphate-bearing minerals. *Am. Min.* **2007**, *92*, 1–18. [CrossRef]
52. Galassi, M.C. *Il disegno svelato*; Ilisso: Nuoro, Italy, 1998; p. 18.
53. Bell, I.M.; Clark, R.J.H.; Gibbs, P.J. Raman spectroscopic library of natural and synthetic pigments (pre- ≈ 1850 AD). *Spectrochim. Acta A.* **1997**, *53*, 2159. [CrossRef] [PubMed]
54. Kirby, J.; Spring, M.; Higgitt, C. The technology of red lake pigment manufacture: Study of the dyestuff substrate. *Natl. Gallery Tech. Bull.* **2005**, *6*, 71–87.
55. Gliozzo, E. Pigments—Mercury-based red (cinnabar-vermilion) and white (calomel) and their degradation products. *Archaeol. Anthropol. Sci.* **2021**, *13*, 210. [CrossRef]
56. Bonizzoni, L.; Bruni, S.; Gargano, M.; Guglielmi, V.; Zaffino, C.; Pezzotta, A.; Pilato, A.; Auricchio, T.; Delvaux, L.; Ludwig, N. Use of integrated non-invasive analyses for pigment characterization and indirect dating of old restorations on one Egyptian coffin of the XXI dynasty. *Microchem. J.* **2018**, *138*, 122–131. [CrossRef]
57. Burgio, L.; Clark, R.J.H. Library of FT-Raman spectra of pigments, minerals, pigment media and varnishes, and supplement to existing library of Raman spectra of pigments with visible excitation. *Spectrochim Acta A* **2001**, *57*, 1491. [CrossRef]
58. Kovala-Demertzi, D.; Papathanasis, L.; Mazzeo, R.; Demertzis, M.A.; Varella, E.A.; Prati, S. Pigment identification in a Greek icon by optical microscopy and infrared microspectroscopy. *J. Cult. Herit.* **2012**, *13*, 107–113. [CrossRef]
59. Higgitt, C.; Spring, M.; Saunders, D. Pigment-medium interactions in oil paint films containing red lead or lead-tin yellow. *Natl. Gallery Tech. Bull.* **2003**, *24*, 75–95.
60. Cardinali, M.; De Ruggieri, M.B.; Falcucci, C. *Diagnostica Artistica. Tracce Materiali per la Storia Dell'arte e per la Conservazione*; Palombi Editori: Roma, Italy, 2007; pp. 49–50, 115–118.
61. Cosentino, A. Effects of different binders on technical photography and infrared reflectography of 54 historical pigments. *Int. J. Conserv. Sci.* **2015**, *6*, 290–291.
62. Sebastianelli, M. Le strutture di sostegno dei dipinti su supporto tessile: I telai. Atti del VII Congresso Nazionale IGIIC (Napoli, Castel Dell'Ovo, 8–10 ottobre 2009). *Lo Stato Dell'arte* **2009**, *7*, 389–399.
63. Guiggi, S. Da Bisanzio alla Russia e all'Italia: Il viaggio dell'icona. Web publication/site Porphyra. *Arte e scienza a Bisanzio* **2010**, *1*, 76. Available online: http://www.porphyra.it/numero-14-arte-e-scienza-a-bisanzio/ (accessed on 13 December 2022).
64. Castelli, C. Tecniche di costruzione dei supporti lignei. In *Dipinti su Tavola. La Tecnica e la Conservazione dei Supporti*; Ciatti, M., Castelli, C., Santacesaria, A., Eds.; Edifir: Firenze, Italy, 1999; p. 60.
65. Timar, M.C.; Gurău, L.; Porojan, M. Wood Species Identification. *Int. J. Conserv. Sci.* **2012**, *3*, 11–22.
66. Uzielli, L. Historical overview of panel-making techniques in Central Italy. In *'The Structural Conservation of Panel Paintings' Proceedings of a Symposium at the J. Paul Getty Museum, 24–28 April 1995*; Dardes, K., Rothe, A., Eds.; Getty Museum: Los Angeles, CA, USA, 1998; p. 114.
67. Romagnoli, M.; Sarlatto, M.; Terranova, F.; Bizzarri, E.; Cesetti, S. Wood identification in the Cappella Palatina ceiling (12th century) in Palermo (Sicily, Italy). *IAWA J.* **2007**, *28*, 109–123. [CrossRef]
68. Mastrotheodoros, G.P.; Beltsios, K.G. On the grounds of post-Byzantine Greek icons. *Archaeometry* **2016**, *58*, 830–847. [CrossRef]
69. Burgio, L.; Clark, R.J.H.; Theodoraki, K. Raman microscopy of Greek icons: Identification of unusual pigments. *Spectrochim. Acta A.* **2003**, *59*, 2371–2389. [CrossRef]
70. Melo, H.P.; Cruz, A.J.; Candeias, A.; Mirão, J.; Cardoso, A.M.; Oliveira, M.J.; Valadas, S. FTIR of calcium sulphate-based preparatory layers. *Archaeometry* **2014**, *56*, 513–526. [CrossRef]

71. Gómez, S.S.; Moya, M.S.A.; Ródriguez, J.L.B.; Sastre, O.C.; Aglio, M.I.B.; Muñoz, A.R. Contribution to the study of grounds for panel painting of the Spanish school in the fifteenth and sixteenth centuries. In *Painting Techniques: History, Materials and Studio Practice, Contributions to the Dublin Congress 7–11 September 1998*; Roy, A., Smith, P., Eds.; International Institute for Conservation of Historic and Artistic Works: London, UK, 1998.
72. Darque-Ceretti, E.; Felder, E.; Aucouturier, M. Foil and leaf gilding on cultural artefacts; forming and adhesion. *Matéria (Rio J.)* **2011**, *16*, 542. [CrossRef]
73. Lobefaro, M. La tecnica esecutiva di base delle icone antiche. In *Lo Stato dell'Arte 1, Atti del I Congresso, Nazionale IGIIC (Torino, Villa Gualino, 5–7 Giugno 2003)*; Il Prato: Saonara, Italy, 2003; pp. 299–304.
74. Lazareff, V.N. Two newly-discovered pictures of the Lucca school. In *The Burlington Magazine for Connoisseurs*; Tatlock, R.R., Ed.; Savile Pub. Co.: London, UK, 1927; Volume 51, pp. 56–67.